

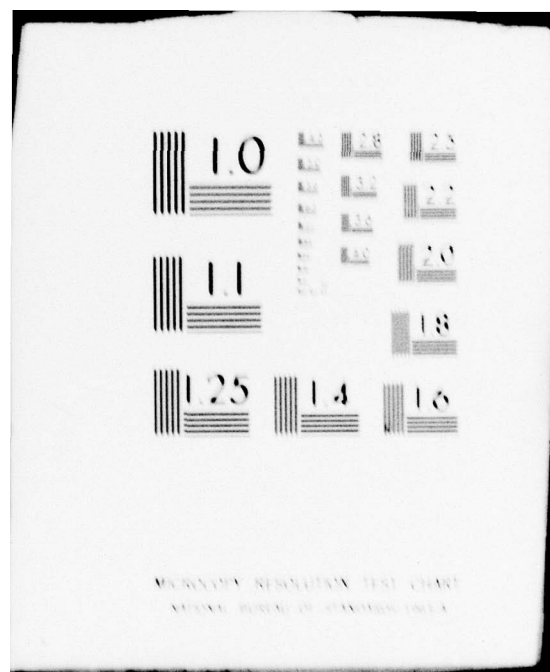
AD-A075 098 ROME AIR DEVELOPMENT CENTER GRIFFISS AFB NY
SPREAD-SPECTRUM DATA LINK TEST FACILITY, (U)
AUG 79 O H MCKEE
UNCLASSIFIED RADC-TR-79-244

F/G 9/5

NL



END
DATE
FILED
3-80
DDC



ADA075098

RADC-TR-79-244

In-House Report

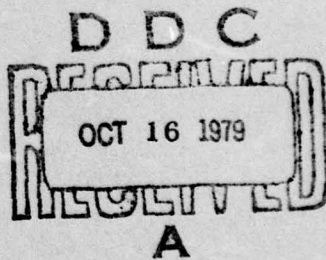
August 1979



SPREAD-SPECTRUM DATA LINK TEST FACILITY

Oscar H. McKee, Capt, USAF

APPROVED FOR PUBLIC RELEASE; DISTRIBUTION UNLIMITED



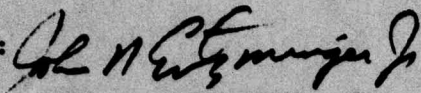
**ROME AIR DEVELOPMENT CENTER
Air Force Systems Command
Griffiss Air Force Base, New York 13441**

79 10 16 076

This report has been reviewed by the RADC Information Office (OI) and is releasable to the National Technical Information Service (NTIS). At NTIS it will be releasable to the general public, including foreign nations.

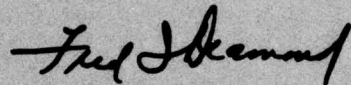
RADC-TR-79-244 has been reviewed and is approved for publication.

APPROVED:



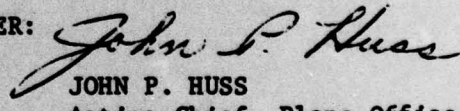
JOHN N. ENTZINGER, JR.
Chief, Location & Control Branch
Communications and Control Division

APPROVED:



FRED I. DIAMOND, Technical Director
Communications and Control Division

FOR THE COMMANDER:



JOHN P. HUSS
Acting Chief, Plans Office

If your address has changed or if you wish to be removed from the RADC mailing list, or if the addressee is no longer employed by your organization, please notify RADC (DCID), Griffiss AFB NY 13441. This will assist us in maintaining a current mailing list.

Do not return this copy. Retain or destroy.

UNCLASSIFIED

SECURITY CLASSIFICATION OF THIS PAGE (When Data Entered)

DD FORM 1 JAN 73 1473

UNCLASSIFIED

SECURITY CLASSIFICATION OF THIS PAGE (When Data Entered)

UNCLASSIFIED

SECURITY CLASSIFICATION OF THIS PAGE(When Data Entered)

was set at 200 watts CW, however, additional power is available at the three ground stations.

Section 2 of the report presents the theoretical calculations used to predict the maximum range expected from each of four data links incorporated in a five station test scenario. The maximum theoretical range was calculated to be 414.3 miles, however, the ranges achieved during actual flight testing were approximately 9 dB below theoretical expectations.

Although time constraints did not allow demonstration of fully automatic control of the five station facility, several test flights in the manual mode were flown. These test flights, which extended over a period of six weeks, demonstrated the ability of the modem to provide a communications link at the desired range and bit error rate.

UNCLASSIFIED

SECURITY CLASSIFICATION OF THIS PAGE(When Data Entered)

PREFACE

This report concerns the development of an in-house data link test facility for evaluating wide bandwidth spread spectrum modems. The work was conducted in the Communications ECCM Techniques Section, Location and Control Branch, Communications and Control Division, Rome Air Development Center, under Job Order Number 55561208 and Job Order Number 22170102.

The author would like to acknowledge the assistance and support of Mr. Stanley Wengyn of the Northern Communication Area, Griffiss AFB NY for fabrication of major portions of the system hardware.

TABLE OF CONTENTS

SECTION	PAGE
1. INTRODUCTION	1
2. DESIGN GOALS	6
3. SYSTEM CONFIGURATION	18
3.1.a Ground Control Station	
3.1.b Sensor Aircraft	
3.1.c Relay Aircraft	
3.1.d Beacon	
3.1.e Moving Target	
4. SUMMARY	43
5. REFERENCES	45

PRECEDING PAGE BLANK - NOT FILMED

LIST OF ILLUSTRATIONS

<u>Figure</u>	<u>Page</u>
1. Flight Scenario	2
2. Block Diagram of Test Scenario	5
3. Cable Attenuation Graph	10
4. Gain Vs Frequency Graph for IF Filter	12
5. Photo of Composite RF Equipment	19
6. Photo of GCS Modem and PDP 11/40	19
7. Photo of GCS Transmitter Tower and Building 817 at Griffiss AFB	20
8. Drawing of GCS Computer Control Flow Diagram	21
9. Drawing of GCS RF Equipment	22
10. GCS Transmitter Schematic (7900 MHz)	23
11. Photo of WCCM Output Waveform	23
12. GCS Receiver at 4900 MHz (Schematic)	24
13. GCS Receiver at 7350 MHZ (Schematic)	24
14. Photo of Typical Transmitter Output Waveform	26
15. Photo of Typical Receiver Passband (Noise Only)	27
16. Photo of Typical Receiver Output with WCCM Waveform	28
17. Sensor Aircraft Control Flow Diagram	30
18. Block Diagram of Sensor Aircraft RF Equipment	31
19. Block Diagram of Relay Aircraft RF Equipment	31
20. Schematic of Sensor Transmitter Unit 7350 MHz	32
21. Schematic of Sensor Receiver Unit at 7900 MHz	32

<u>Figure</u>		<u>Page</u>
22.	Schematic of Sensor Receiver Unit at 4500 MHz	33
23.	Schematic of Relay Transmitter 4900 MHz	33
24.	Schematic of Relay Receiver at 7900 MHz	34
25.	Schematic of Relay Receiver at 4500 MHz	34
26.	Antenna Pattern for Button Antennae Used on Both Aircraft for Transmit and Receive	35
27.	Block Diagram of Beacon RF Equipment	36
28.	Photograph of Interior of Relay Aircraft with Equipment Installed	37
29.	Photograph of Relay Aircraft Exterior	37
30.	Photograph of Relay Aircraft Exterior Showing Close-up of Button Antennae	38
31.	Schematic Drawing of Beacon Transmitter Unit	39
32.	Schematic Drawing of Beacon Receiver	39
33.	Block Diagram of Target RF Equipment	40
34.	Photograph of Van Used as Moving Target	41
35.	Schematic Drawing of Target Transmitter	42
36.	Schematic Drawing of Target Receiver 4900 MHz	42

LIST OF TABLES

1.	Link Theoretical Range Computation	16
2.	Summary of Link Functions	17

1. INTRODUCTION

1.1 The purpose of this technical report is to define the microwave receiving and transmitting section of a data link test facility developed by RADC personnel at Griffiss AFB NY. This report will also serve as an operating manual for future users of the test facility.

1.2 The objective and design goals of the test facility were to provide a versatile test bed for evaluating advanced state-of-the-art data link modems. The equipment developed operates at an intermediate frequency of 300 MHz and a nominal 3dB bandwidth of 100 MHz. Four RF frequencies were used in the present configuration to link the five stations. Additional details on the technical and operational parameters of the test bed will be provided in subsequent sections of the report.

1.3 Conceptually the test facility is designed to be as general as possible to allow the testing of many generically different modems; however, for this report emphasis will be placed on the facility being used in conjunction with an experimental spread spectrum modem designed and built to RADC specifications by Hughes Aircraft Corporation, Fullerton, California.

This modem, known as the Wideband Command and Control Modem (WCCM),¹ and the test facility were to be incorporated to form a data distribution network for the Multilateration Radar Surveillance and Strike System (MRS³) being tested at RADC. Figure 1 is a block diagram of the test scenario showing the three ground stations and two airborne stations. The abbreviations in parenthesis are: C & C, Command Control; V & T, Video and Telemetry; TDMA, Time Division Multiple Access; V, Video; GB, Ground Beacon; GCS Ground Control Station and MT, Moving Target.

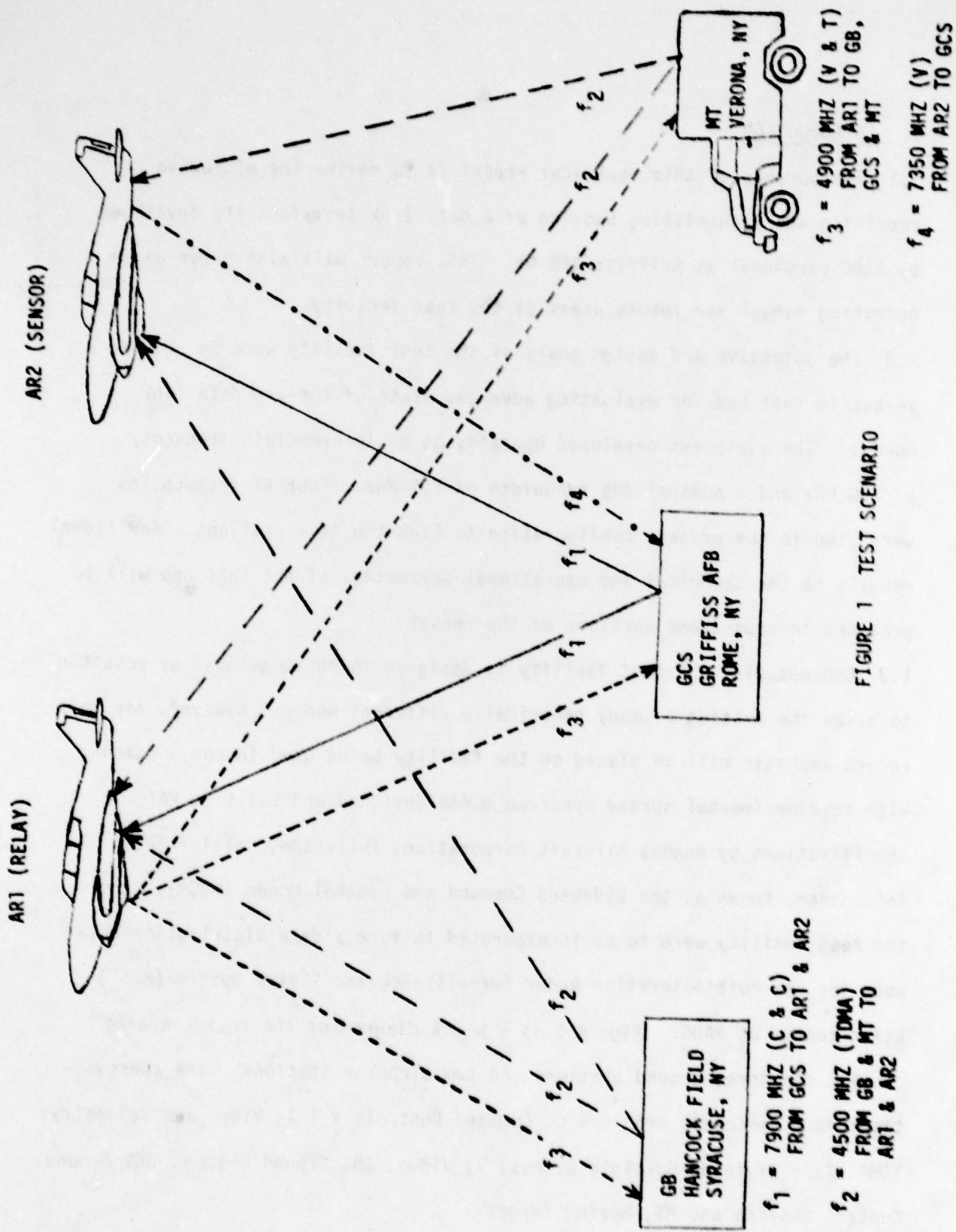


FIGURE 1 TEST SCENARIO

1.4 The objective of the MRS³ test was to demonstrate the ability of an airborne phased array radar to pinpoint the location of slowly moving ground targets such as tanks and truck convoys. The WCCM was selected as the data link for the test because of its high data rate, 40 megabits per second maximum, and also its inherent ability to perform accurate position location.² The position location accuracy of the modem is a function of the direct sequence keying rate of 60 megachips per second. At 60 megachips the range resolution is approximately 17 feet. The position of the two aircraft was obtained by making a range measurement from the GCS and the GB to both aircraft. Given the altitude of the aircraft and these two range measurements, each aircraft could be located quite accurately, (employing an altitude assisted bilateration technique and an algorithm in the GCS computers). Once the aircraft positions were known, the same technique could be employed to determine the position of the moving target using the aircraft as the reference point. The value obtained for the moving target could then be compared with the value obtained from the radar carried on board the sensor aircraft. Theoretically, the value obtained from the data link would be more accurate than the radar.

1.5 Of course, the main purpose of the data link was to relay data to all five stations in the test scenario. Command data was transmitted from the GCS to the two airborne platforms, with radar and target position information transmitted to the ground. A third function of the data link was to provide position location update information to the inertial navigation equipment of the sensor aircraft. Once again, this technique is used because of the data link's ability to accurately determine a cooperating platform's

position. With greater position accuracy, the radar target data would also be more accurate.

1.6 Figure 2 is a scaled drawing of the geographical layout of the MRS³ flight test scenario. The flight path for the two aircraft was an ellipse with a major axis of 15 miles, and a minor axis of three nautical miles. The shaded area is the area where the three dB beamwidths of the ground antennae overlapped. The antennae were all standard design horn antennae. The beacon and target transmitted at 4500 MHz, the Ground Station at 7900 MHz, thus the difference in beamwidths. The GCS beamwidth was approximately 20 degrees at the half power points, the beacon and target were approximately 32 degrees at the half power points.

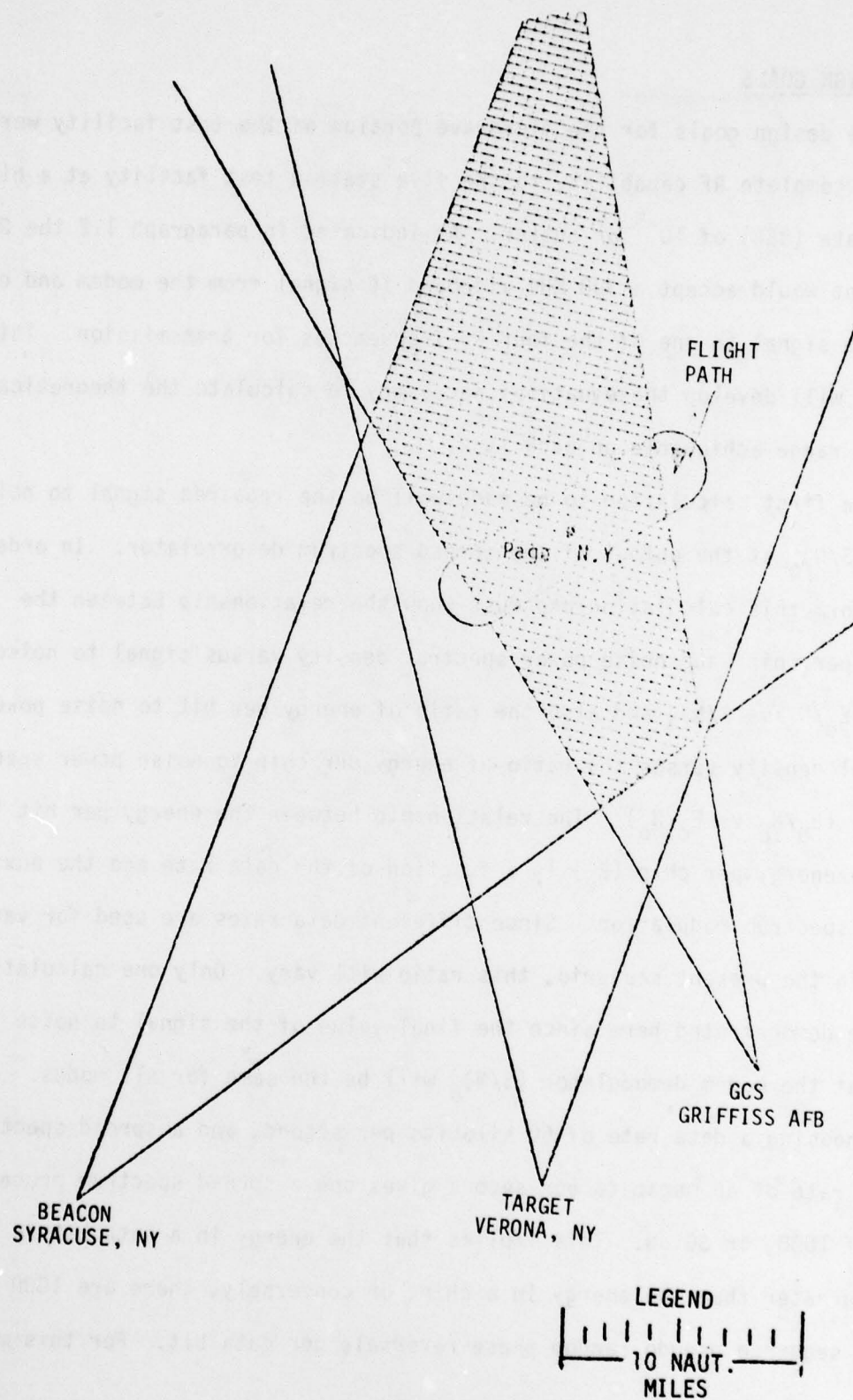


FIGURE 2 GEOGRAPHICAL LAYOUT

2. DESIGN GOALS

2.1 The design goals for the microwave portion of the test facility were to provide complete RF capability to the five station test facility at a bit error rate (BER) of 10^{-5} or better. As indicated in paragraph 1.2 the RF equipment would accept a 300 MHz wideband IF signal from the modem and convert the signal to one of the four RF frequencies for transmission. This section will develop the equations necessary to calculate the theoretical maximum range achievable on each link.

2.2 The first calculation to be made will be the required signal to noise ratio (S/N)₀ at the output of the spread spectrum decorrelator. In order to perform this calculation one must know the relationship between the energy per chip and noise power spectral density versus signal to noise ratio (E_c/N_0 vs S/N), and also the ratio of energy per bit to noise power spectral density versus the ratio of energy per chip to noise power spectral density (E_b/N_0 vs E_c/N_0). The relationship between the energy per bit (E_b) and the energy per chip (E_c) is a function of the data rate and the auxiliary spread spectrum modulation. Since different data rates are used for various links in the present scenario, this ratio will vary. Only one calculation will be demonstrated here since the final value of the signal to noise ratio at the modem demodulator (S/N)₀ will be the same for all modes.

2.3 Choosing a data rate of 60 kilobits per second, and a spread spectrum keying rate of 60 megabits per second gives one a spread spectrum processing gain of 1000, or 30 dB. This implies that the energy in a data bit is 1000 times greater than the energy in a chip, or conversely, there are 1000 direct sequence pseudo random phase reversals per data bit. For this mode

of operation for the WCCM at 10^{-5} BER requires an E_b/N_0 of 12 dB. The S/N calculation is presented below³:

E_c = energy per PN chip

N_0 = noise power spectral density

E_b = energy per data bit

PG = spread spectrum processing gain

$(S/N)_i = S/N$ ratio at demodulator input

$(S/N)_o = S/N$ ratio at demodulator output

$$(S/N)_i = \frac{16}{\pi^2} \cdot \frac{E_c}{N_0}$$

$$E_b = 1000 E_c$$

$$\frac{E_b}{N_0} = 10^3 \frac{E_c}{N_0} \rightarrow \frac{E_c}{N_0} = 10^{-3} \frac{E_b}{N_0}$$

$$(S/N)_i = \frac{16}{\pi^2} \cdot 10^{-3} \frac{E_b}{N_0}$$

$$10 \log (S/N)_i = 10 \log \frac{(16)}{(\pi^2)} + 10 \log 10^{-3} + 10 \log E_b/N_0$$

$$\text{for WCCM @ BER of } 10^{-5} \rightarrow E_b/N_0 = +12 \text{ dB}^4$$

$$(S/N)_i \text{ dB} = 2.1 + 12 - 30 = -15.9 \text{ dB}$$

$$(S/N)_{o \text{ dB}} = PG + (S/N)_i = 30 \text{ dB} - 15.9 \text{ dB}$$

$$(S/N)_o = 14.1 \text{ dB}$$

It was necessary to calculate the S/N ratio for the modem in order to determine the maximum range achievable. Range calculations will be presented in Section 2.5. The above calculation is required since S/N is not normally used when plotting BER information. The energy per bit (E_b) is used for BER plotting in order to allow one to compare the performance of various modulation schemes with equivalent energy per information rate. With S/N the energy per information rate varies with different modulation schemes.

2.4 With the S/N information now available, the remaining parameters necessary to determine the maximum range for the various links will be calculated. The other parameters required are the minimum discernable signal (MDS) for the receivers, antenna gain, and the processing gain for the various data rates. Of course the maximum range that will be determined theoretically will not be achievable during the actual flight tests. The values determined mathematically do not take into consideration the dynamic properties of the channel (multipath and fading) and the inability to maintain the transmitting and receiving antennae on boresight. However, it does allow one to determine if the approach to be attempted is within the realm of possibility. The processing gain for the various links are as follows:

a. C & C $\frac{60 \text{ MHz}}{40 \text{ KHz}} = 31.76 \text{ dB}$

b. Telemetry $\frac{60\text{MHz}}{2400 \times 6} = 36.2 \text{ dB}$

c. TDMA $\frac{60\text{MHz}}{40 \text{ KHz}} = 31.76 \text{ dB}$

$$d. \text{ Video} \quad \frac{40\text{MHz}}{5 \text{ MHz}} = 9\text{dB}$$

2.3 The last parameter needed in order to perform the range calculations is the noise figure of the receivers.

The noise figure equation of cascaded elements is:⁵

$$F_0 = F_1 + \frac{F_2 - 1}{G_1} + \frac{F_3 - 1}{G_1 G_2} + \frac{F_4 - 1}{G_1 G_2 G_3} + \dots +$$

For the receivers built for the MRS³ testing the following data applies:

F_0 = system noise factor

NF = system noise figure = $10 \log F_0$

L_1 = 4 dB = 2.51 (approximately 10 feet of RG 214 cable, see Fig 3)

L_2 = 1.5 dB = 1.4 (insertion loss of preselector filter)

F_3 = 5 dB = 3.16 (noise figure of pre-amp)

F_4 = 1 dB = 1.26 (insertion loss of isolator)

G_1 = $1/L_1$ = $1/(2.51)$ = (loss due to cable) where $G = 1/L$

G_2 = $1/L_2$ = $1/(1.4)$ = (loss due to preselector)

G_3 = 32 dB Gain of pre-amp

$$F_0 = 2.51 + \frac{1.4-1}{1/2.51} + \frac{3.16-1}{(1/2.51)(1/1.4)} + \frac{1.26-1}{(1/2.51)(1/1.4)(1600)}$$

$$F_0 = 2.51 + (.9)(2.51) + (2.16)(3.51) + \frac{(.26)(3.51)}{1600} + \dots +$$

$$F_0 = 2.51 + 1.04 + 7.58 + 0.00057$$

$$F_0 = 11.13$$

$$\text{NF} = 10 \log 11.13 = 10.46 \text{ dB}$$

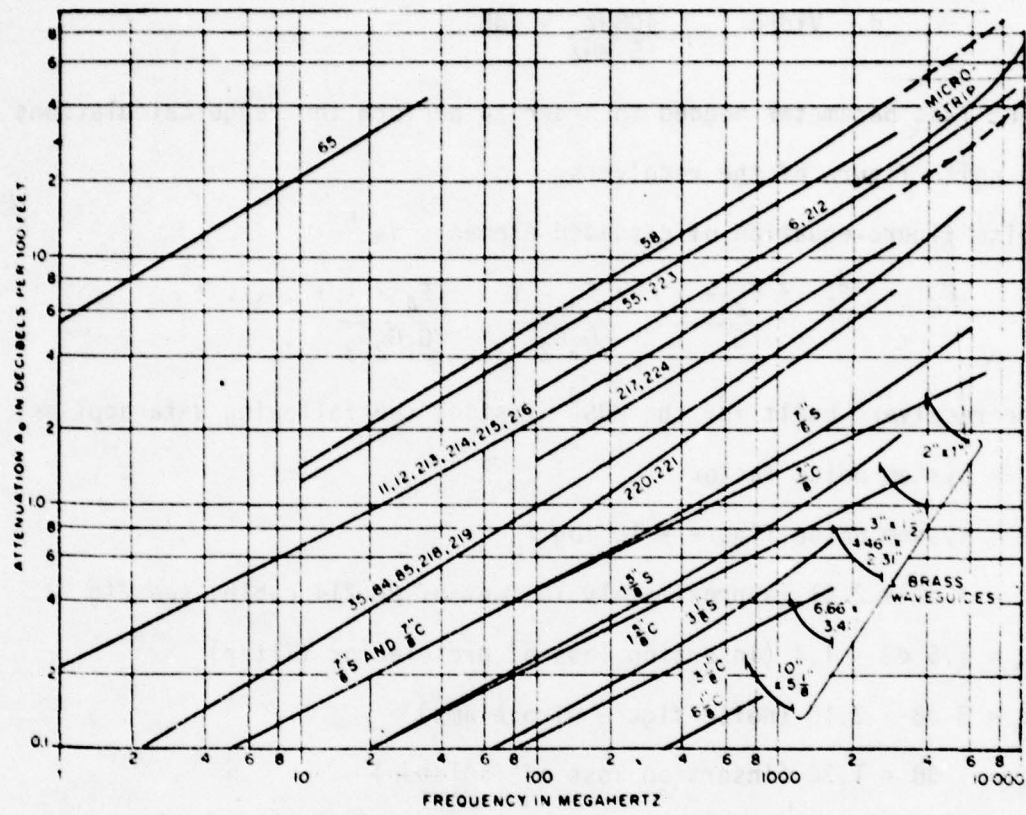


FIGURE 3 CABLE ATTENUATION⁶

The noise figure equation was truncated after the fourth stage since the gain of the preamp (G_3) makes the following factors negligible.

2.4 The noise figure of the receivers was also measured in the lab. The procedure used to obtain the noise figure of the receivers was to measure the total noise power output from the receiver, measure the total receiver gain and the IF bandwidth and use the following equation:

$$N_0 = KTBGF$$

$$N_0 \text{ (dB)} = KTB \text{ (dB)} + G \text{ (dB)} + F \text{ (dB)}$$

$$F \text{ (dB)} = N_0 \text{ (dB)} - KTB \text{ (dB)} - G \text{ (dB)}$$

VALUES USED FOR NOISE FIGURE MEASUREMENT:

$$T = 290^{\circ} \text{ Kelvin}$$

$$B = \text{IF Bandwidth} = 103 \text{ MHz}$$

$$G = \text{Receiver gain} = 43.14 \text{ dB}$$

$$K = \text{Boltzman's constant} = 1.38 \times 10^{-23} \text{ joules/degree Kelvin}$$

$$N_0 = -42.40 \text{ dBm}$$

$$KTB = 1.38 \times 10^{-23} \times 290 \times 1.03 \times 10^8 \frac{\text{watts}}{\text{Hz}}$$

$$KTB = 4.15 \times 10^{-13} \frac{\text{watts}}{\text{Hz}}$$

$$KTB = 4.15 \times 10^{-10} \frac{\text{milliwatts}}{\text{Hz}}$$

$$KTB = -93.83 \text{ dBm}$$

Plugging these values into the equation on page 10 yields:

$$F(\text{dB}) = -42.40 \text{ dBm} + 93.83 \text{ dBm} - 43.14 \text{ dB}$$

$$F(\text{dB}) = 8.29 \text{ dB}$$

The bandwidth of the receiver was obtained by analyzing the IF filter on an HP network analyzer. Figure 4 is a printout of the gain vs frequency response of the filter. Since the filters used in the IF of all receivers were 11 pole Chebychev filters, the 3 dB bandwidth is extremely close to the required noise bandwidth for our calculations. The bandwidth obtained from Figure 4 is 103 MHz.

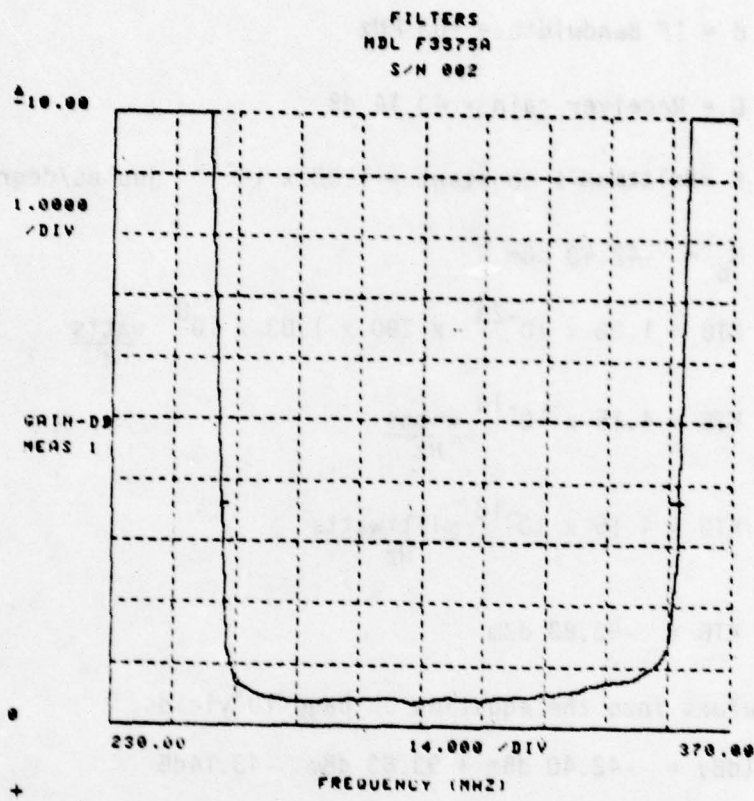


FIGURE 4 IF FILTER BANDPASS CHARACTERISTICS

The measured and calculated values for the noise figure are 8.29 and 10.46 dB respectively. The difference between measured and calculated values can be attributed to the use of the manufacturers nominal value for all components in the theoretical calculation.

2.5 With all of the necessary information now at hand, the maximum theoretical range can be calculated for the various links of the MRS³ flight scenario. The maximum range achievable is a function of the power transmitted, free space attenuation, receiver sensitivity, noise figure, system losses, required S/N for 10^{-5} BER, antenna gain, and frequency. The equation used to obtain the maximum range is:⁷

$$R = \left[\frac{P_t G_t G_r \lambda^2 (PG)}{(4\pi)^2 (S/N) (KTBF) L} \right]^{1/2}$$

P_t = RMS average power transmitted

G_t = Transmitting antenna gain

G_r = Receiving antenna gain

λ = Wave length

PG = Processing gain

S/N = Required signal to noise ratio for 10^{-5} BER

KTBF = Thermal noise level of receiver

F = Receiver noise figure

L = System losses

The rational behind using this particular equation is based on the following analysis:

a. Power density at the receiver $P_r = \frac{P_t G_t}{4\pi R^2} = \text{watts meter}^2$

$$\frac{R^2 = \frac{P_t G_t}{4\pi P_r}}{P_r = \text{Receiver Power}}$$
$$P_n = \text{Noise power}$$

b. P_r can be written as $\frac{S}{N} = \frac{P_r}{P_n}$ in order to make the equation more useful to our needs. $P_n = kTB$, thus $-P_r = (S/N)kTB$

c. This gives us the following equation for the maximum range without the receiving antenna gain being taken into consideration.

$$\frac{R^2 = \frac{P_t G_t}{4\pi (S/N) KTB}}$$

d. The maximum range achievable will naturally be a function of the gain of the receiving antenna; however, one cannot just multiply the gain of the receiving antenna times the value obtained in step 2.5.c above. The parameter needed at this point is the effective capture area of the receiving antenna which is found from the following equation:

$$G_r = \frac{4\pi A_e}{\lambda^2} \quad \text{where } A_e = \text{effective area of antenna.}$$

e. We can now take the receiving antenna gain into consideration for our calculation of the maximum range equation.

$$R^2 = \frac{P_t G_t A_e}{4\pi (S/N) kTB} = \frac{P_t G_t G_r \lambda^2}{(4\pi)^2 (S/N) kTB} \text{ meters}^2$$

f. The only parameters remaining which need to be taken into consideration are the system losses (L), processing gain (PG) and the receiver noise figure (F). Once this is done we obtain the equation presented in paragraph 2.5. :

$$R = \left[\frac{P_t G_t G_r \lambda^2 (PG)}{(4\pi)^2 (S/N) (KTBF) L} \right]^{1/2}$$

The maximum theoretical ranges calculated for the four links used in the MRS³ flight test scenario are tabulated below in Table 1.

	LINK 1 (7900 MHZ) GCS TO ART & AR2		LINK 2 (4500 MHZ) GB & MT TO ART & AR2		LINK 3 (7350 MHZ) AR2 TO GCS		LINK 4 (4900 MHZ) ART TO GCS, GB, MT	
	+	-	+	-	+	-	+	-
P _t dBm	43		43		43		43	
G _t dB	16		16		15.5		7	
G _r	7		7		17		17	
$\lambda^2 = \left(\frac{C}{f}\right)^2$		28.4		23.5		27.8		24.26
P _G	31.76		31.76		9		36.2	
$(4\pi)^2$		21.9		21.9		21.9		21.9
S/N		14.1		14.1		14.1		14.1
KTB _F	83.54		83.54		83.54		83.54	
L		13		10		9		10
R ² dB-m ²	103.9		111.8		95.24		116.98	
R dB-m	51.95		55.9		47.62		58.24	
R km	156.67		389.0		57.80		666.8	
R MILES	97.35		241.7		35.9		414.3	

TABLE 1 LINK RANGE CALCULATIONS

<u>LINK</u>	<u>FREQUENCY</u>	<u>DATE RATE</u>	<u>PROCESSING GAIN (PG)</u>	<u>MAXIMUM THEORETICAL RANGE (NAUTICAL MILES)</u>
<u>CBC</u>				
GCS To ARI & AR2	7900 MHz	40KHz	31.76dB	97.35
<u>TDMA</u>				
GR to ARI & AR2	4500 MHz	40KHz	31.76dB	241.70
MT to ARI & AR2	4500 MHz	40KHz	31.76dB	241.70
<u>VIDEO</u>				
ARI to RCS	7350 MHz	5MHz	9dB	35.9
<u>TELEMETRY</u>				
ARI to GCS, GR, MT	4900 MHz	14.4 KHz	36.2dB	414.3

TABLE 2 SUMMARY OF LINK FUNCTIONS

3. SYSTEM CONFIGURATION

3.1 As indicated in Figure 2, the MRS³ test scenario required five geometrically separated stations. This section will cover in detail each of the stations, pinpointing their capabilities and similarities.

a. Ground Control Station (GCS)

1. The ground control station must maintain contact with the two airborne platforms (AR1 & AR2) at all times for command and control purposes. Also, the computers in the GCS maintained complete control of the data link portion of the entire scenario at all times.

a. Equipment at the GCS consisted of:

1. PDP 11/40 computer
2. PDP 11/20 computer
3. GCS modem
4. Microprocessor interface units
5. Transmitter/receiver and antenna assembly.

2. The ground control station was housed in Building 817 at Griffiss AFB, with the transmitting and receiving antennae being mounted on a 30-foot tower adjacent to the building. Figure 5 is a photograph of all the microwave equipment prior to being installed in their respective locations. Figure 6 is a photograph of the GCS modem with the PDP 11/40 computer immediately to its right. Figure 7 is a photograph of the 30-foot tower adjacent to the building showing the three horn antennae used for transmitting and receiving. The antennae are mounted on a remotely controlled mast that can be rotated 360° in azimuth from inside the building.

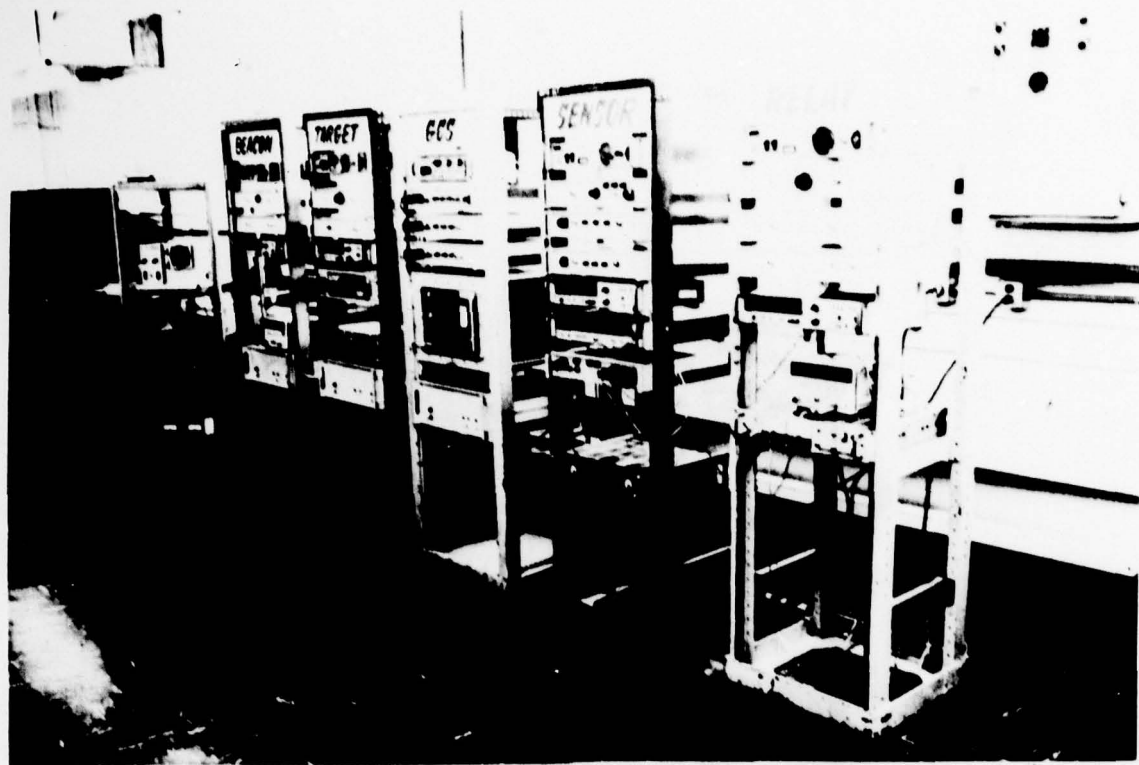


FIGURE 5 RF MICROWAVE EQUIPMENT

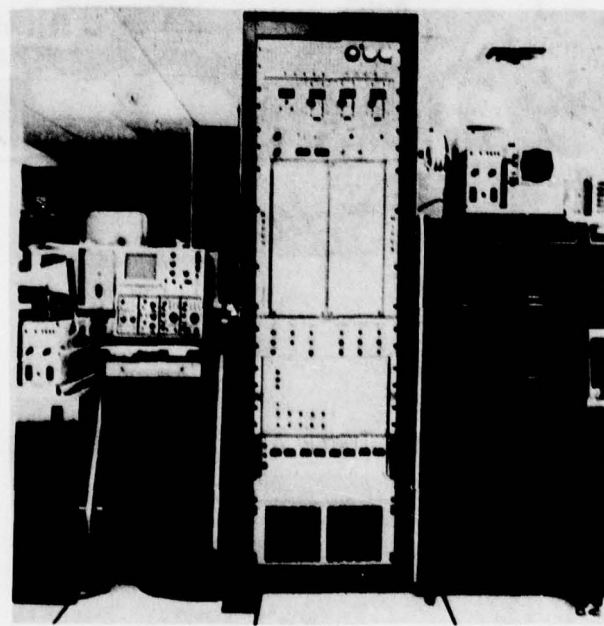


FIGURE 6 GCS MODEM AND PDP 11/40 COMPUTER



FIGURE 7 30-FOOT TOWER AT BUILDING 817 (GCS)

3. Figure 8 is a schematic drawing of the microprocessor interface units developed for interfacing the flow of data between the various computers used during the flight test operation. Additional information may be obtained on the computer control and interfacing functions by referring to another RADC technical report to be published by Mr. Dan Patterson and Lt Steve Hettinger from the Active Location and Control Section of the Location and Control Branch at RADC.

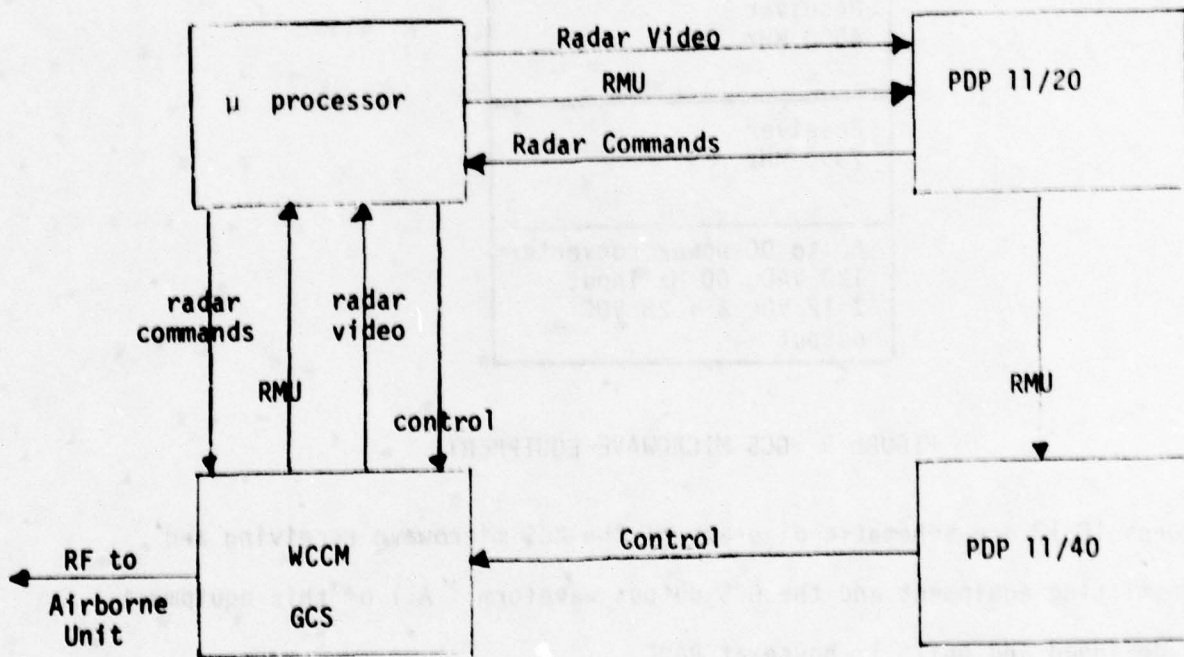


FIGURE 8 MICROPROCESSOR INTERFACE

4. The GCS microwave equipment consisted of a transmitter unit and its high power traveling wave tube amplifier (TWTA), two receiver units and a power supply box.

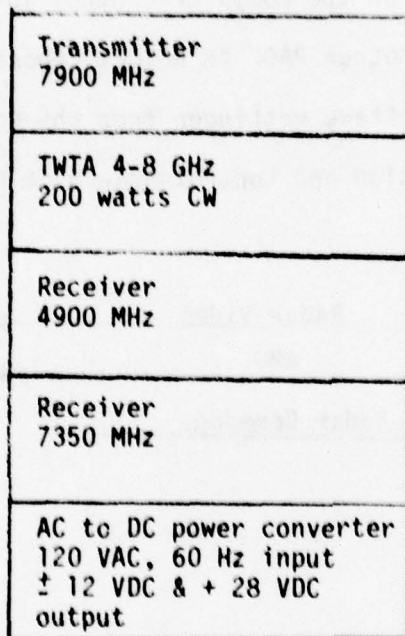


FIGURE 9 GCS MICROWAVE EQUIPMENT

Figures 10-13 are schematic diagrams of the GCS microwave receiving and transmitting equipment and the GCS output waveform. All of this equipment was designed and built in-house at RADC.

a. The design goal for the transmitter sections for all of the units was to take the wideband IF signal from the WCCM at 300 MHz and a nominal RMS power level of 0 dBm and up-convert it to the microwave region for transmission. The 60 Megachip Continuous Phase Shift Modulation (CPSM)* waveform gave the output signal a null to null bandwidth of 90 MHz.

*CPSM is a Hughes Aircraft implementation of a SQPSK modulation scheme. For more details see reference 1.

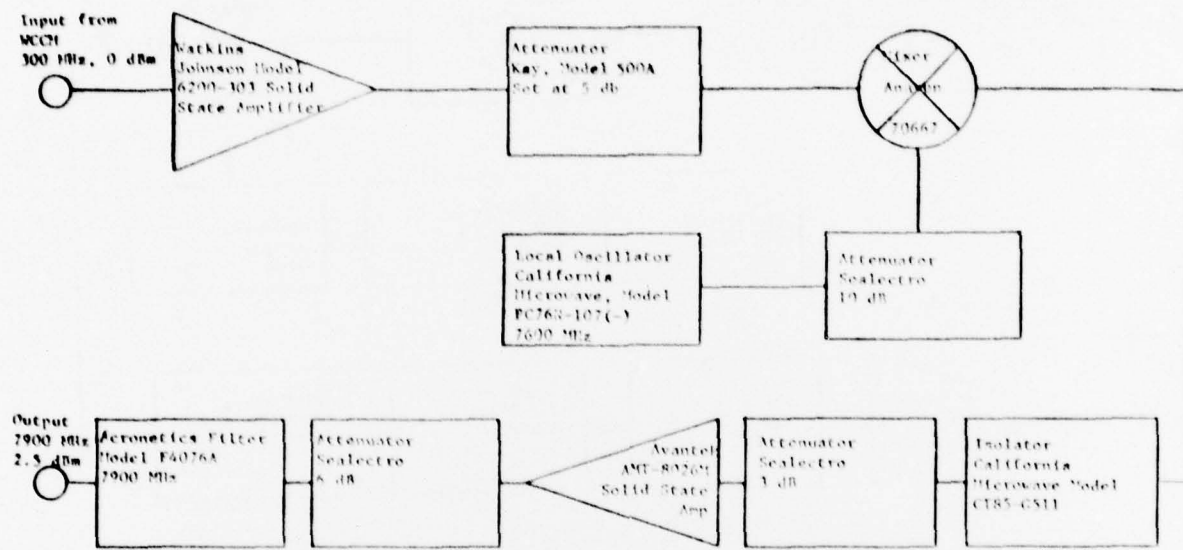


FIGURE 10 GCS TRANSMITTER 7900 MHZ

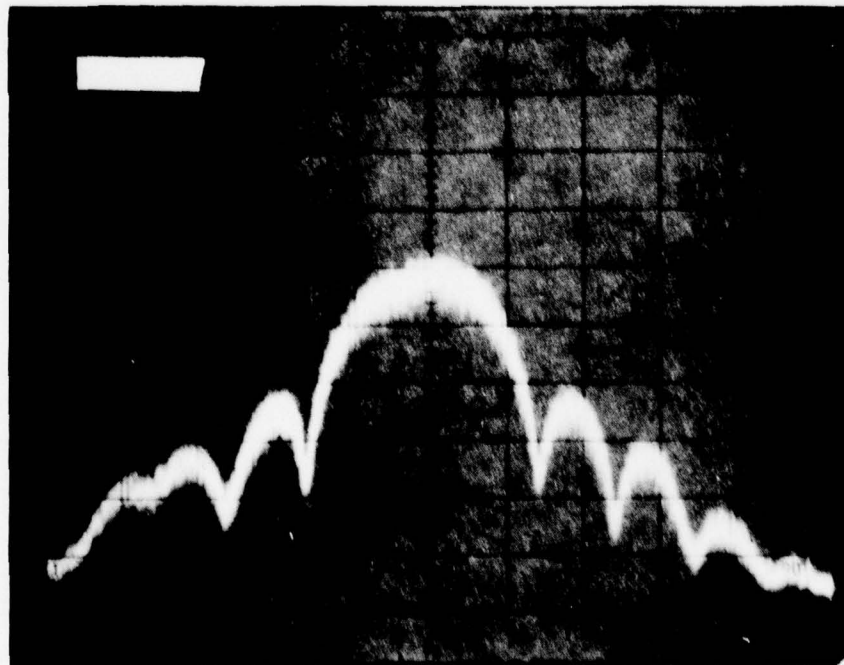


FIGURE 11 GCS MODEM OUTPUT

$F_Q = 300 \text{ MHz}$
 IF BW = 1 MHz
 SCANWIDTH = 30 MHz/DIV
 VERTICAL SCALE = 10 dB/DIV
 SCAN TIME = 3 millisecond/SWEEP

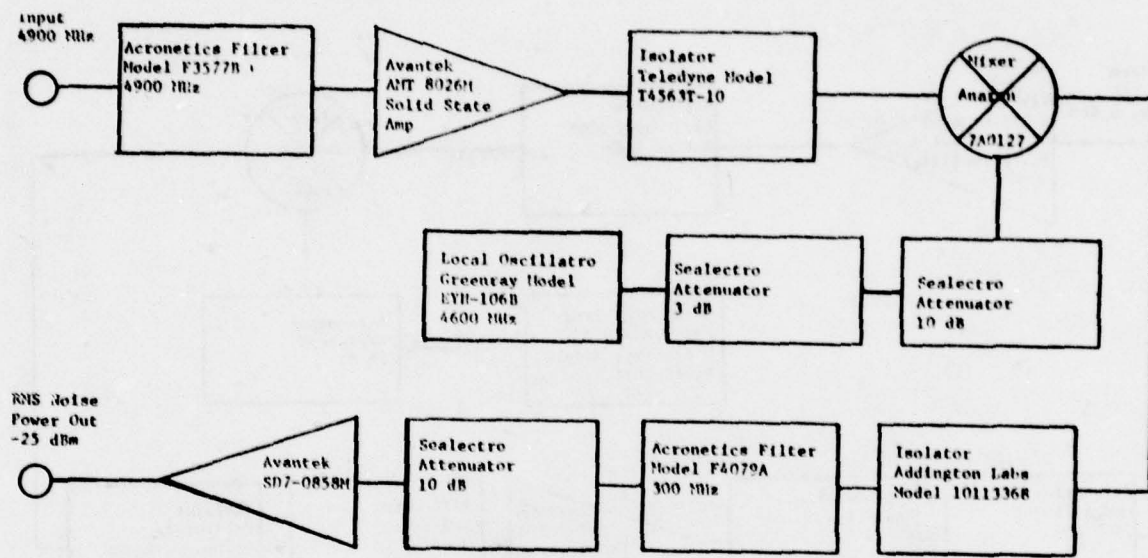


FIGURE 12 GCS RECEIVER 4900 MHZ

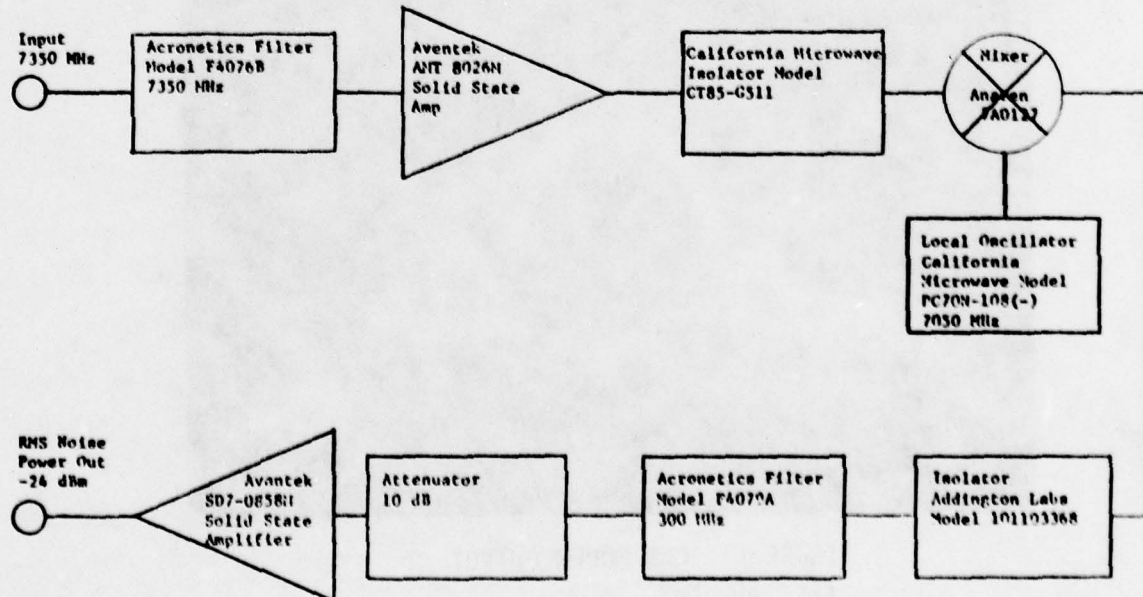


FIGURE 13 GCS RECEIVER 7350 MHZ

The GCS transmitter section takes the wideband IF signal and multiplies it in frequency to 7900 MHz in a single stage multiplication process. In Figure 10, the solid state amplifier and attenuator at the input serve to set the signal level to the balanced modulator at the prescribed level. The local oscillator at 7600 MHz combines with the WCCM waveform to produce the desired 7900 MHz signal at the modulator output. All oscillators incorporated into the RF equipment had a stability of ± 2 parts in 10^{-8} per hour. The isolator at the modulator output was required to diminish the effects of a mismatch condition that existed between the mixer and the solid state amplifier that was to follow it. The result of adding the isolator was a vast reduction in the spurious frequency components that were being experienced in the passband. The signal which is sent to the output bandpass filter is spectrally free of spurious components. The output filter passes essentially only the main lobe of the spread spectrum waveform, and reduces the possibility of intermodulation occurring in the final high power TWT. The passband of the output filter is nominally 100 MHz, with the out of band signal being down by 60 dB at frequencies greater than 500 MHz from the center frequency. See Figures 11 and 14.

b. Both of the GCS receivers were designed with the same basic requirements, they differ essentially only in their frequency band of operation. The input filter of the receivers is of the same design as the output filter of the transmitter, i.e. they are all 11 pole Chebychev filters with phase linearity requirements of ± 10 degrees over the entire passband. The parameters on the filters (especially passband characteristics) were made very stringent since it was known that the transmitting and receiving antennae would all be colocated. During the considerable testing that has



FIGURE 14
TRANSMITTER OUTPUT

$F_0 = 4500$ MHz
IF BW = 1 MHz
SCANWIDTH - 30 MHz/DIV
VERTICAL SCALE - 10 dB/DIV
SCAN TIME - 3 MSEC/SWEEP

been done to date, no antenna cross talk problems have been experienced on any of the platforms. The receivers, as in the transmitters, are single stage down conversion process. The incoming signal is combined with the local oscillator to produce the required 300 MHz IF that is to be sent to the modem. Of course, one of the main design goals with the receivers was to minimize the equipment noise figure. This was accomplished by placing the high gain-low noise figure solid state amplifier as close to the front end of the receiver as possible. The preselection filter had to be placed ahead of the amplifier in order to diminish the effects of the transmitted signal which was colocated on the same mast as most of the receiving antennae. A second primary design goal was to deliver a total signal plus noise power that was within the dynamic range of the modem. This was accomplished by

setting the total noise power level out of receivers at the lower end of the modem AGC range. Any signal level that exceeded this setting would be AGC controlled by the modem. A second AGC circuit was added to the IF amplifier stage of the receivers units. This AGC effort was accomplished by using a PIN diode modulator. The range of controls for the diode were 0 to 5 VDC that produced an attenuation factor of 0 to 40 dB. The control voltage for the AGC was derived from the WCCM AGC circuitry. Figures 15 and 16 are photographs of the passband characteristics of a representative receiver unit with and without an input signal.

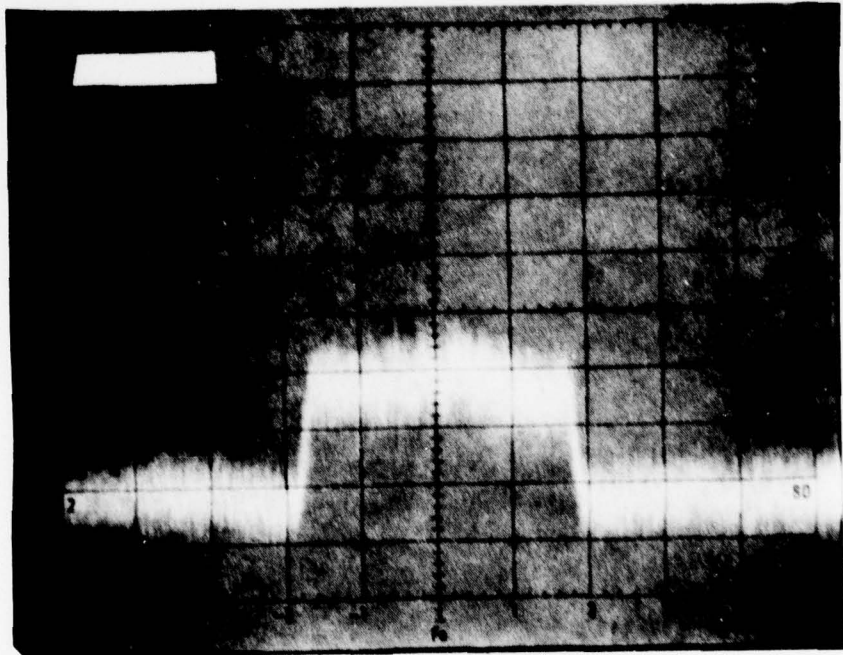


FIGURE 15 RECEIVER PASSBAND

$F_0 = 300 \text{ MHz}$
IF BW = 1 MHz
SCAN WIDTH - 30 MHz/DIV
VERTICAL SCALE - 5 dB/DIV
SCAN TIME - 3 millisecond/SWEEP

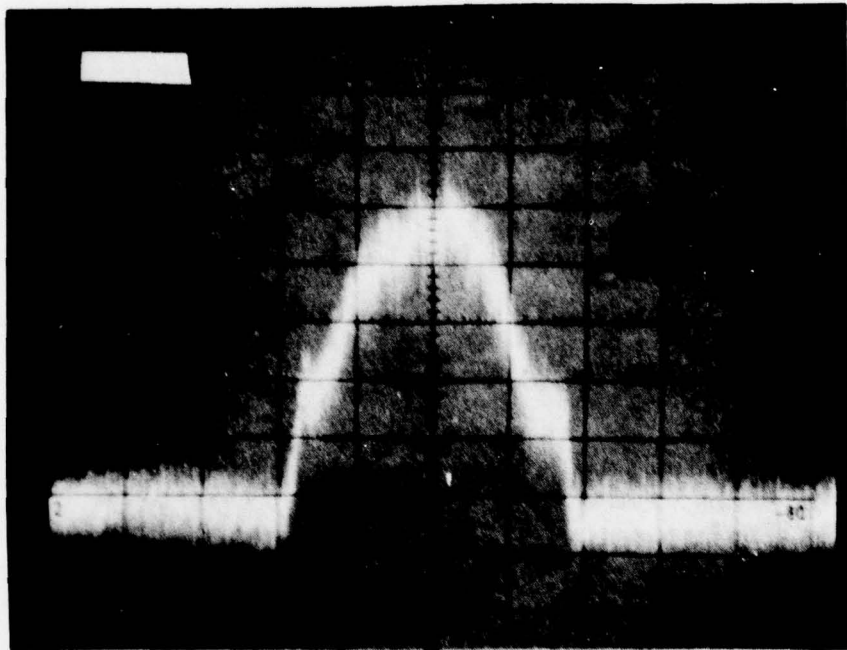


FIGURE 16 RECEIVER OUTPUT

$F_0 = 300 \text{ MHz}$
IF BW = 1 MHz
SCAN WIDTH = 30 MHz/DIV
VERTICAL SCALE = 5 dB/DIV
SCAN TIME = 3 millisecond/SWEEP

b. Sensor aircraft (AR2)

1. The sensor aircraft housed the Multiple Antenna Surveillance Radar (MASR) system that formed the core of the Multilateration Radar Strike Surveillance System test program. The objective of the MRS³ program was to demonstrate the ability of an airborne radar to accurately detect slowly moving ground targets such as tanks and truck convoys. The purpose of the WCCM for these tests was two-fold, first to provide a data link for command and control of the airborne platforms, and secondly to provide improved position location data to the sensor aircraft's internal navigation system. This was accomplished by using the distance measuring aspect of the modem through a bilateration scheme based upon time of arrival of RF pulses from known ground locations. Knowing the aircraft's altitude and the range from the two ground stations, the GCS can determine the aircraft position to within \pm 5 feet. With the aircraft accurately located, the MASR can then more accurately pinpoint the location of the ground targets. For this particular project the target also had receiving and transmitting equipment to make a comparison (position of target) with the radar. Theoretically, the WCCM should be able to pinpoint the target to a much greater degree of accuracy than the radar. Figure 17 is a drawing of the sensor control flow diagram.

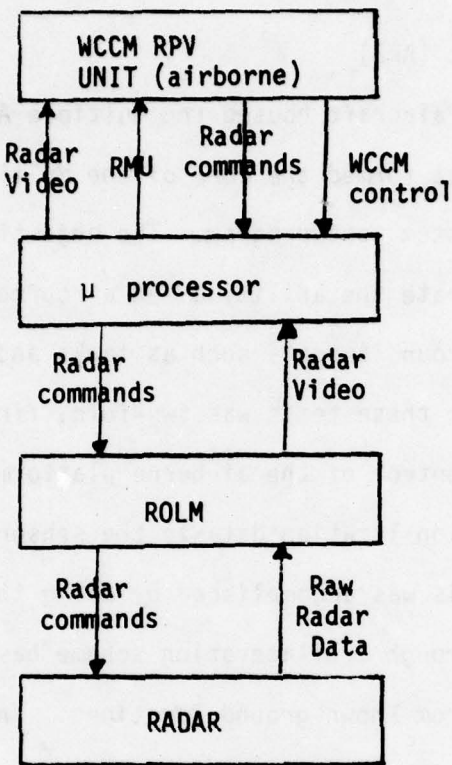


FIGURE 17 SENSOR CONTROL FLOW DIAGRAM

2. The sensor microwave equipment contained one transmitter unit and two receiver units as did the GCS. The design goals for these units were the same as for the GCS (see Figure 18). The ± 5 VDC indicated in Figure 19 is one difference - this voltage was required on the sensor aircraft to power the microprocessor units. Figures 20-22 are schematic drawings of the receiver/transmitter units for the sensor aircraft.

Transmitter Unit 4900 MHz
TWTA 4 - 8 GHz +28 VDC prime power 20 watt CW output
Transmitter Unit 4500 MHz
Transmitter Unit 7900 MHz
DC - DC +28 in \pm 12, + 28 out

FIGURE 19
RELAY MICROWAVE EQUIPMENT

Transmitter unit 7350 MHz
TWTA 4 - 8 GHz +28 VDC prime power 20 watt CW output
Receiver unit 7900 MHz
Receiver unit 4500 MHz
DC to DC converter +28VDC in \pm 12, \pm 5, +28 VDC output

FIGURE 18
SENSOR MICROWAVE EQUIPMENT

c. Relay Aircraft (AR1)

1. The same design goals were required for the relay aircraft equipment as for the sensor aircraft. In Figure 19 note the power supply unit has only \pm 12 VDC and + 28 VDC capability. Also, an additional 6 dB attenuator must be placed external to the transmitter unit input since the output level from the WCCM RPV unit was slightly higher than anticipated. See Figures 23-25 for schematics of the relay aircraft microwave equipment.

2. The antennae used on the relay and sensor aircraft for the data link had a nominal gain of 7 dB. The pattern was uniform in azimuth with a "null" in the pattern when looking nadir to the aircraft. Two different antennae were used for the testing, one tuned for 4-5 GHz, the other tuned to 7-8 GHz. Figure 26 is a representative pattern for the antennae that was run on the Precision Antenna Measurement system at RADC. For reference, an isotropic antenna with unity gain is indicated by the smooth curve inside the data points for the antenna under test. The scale factor is 1 dB per unit, or 5 dB per major unit.

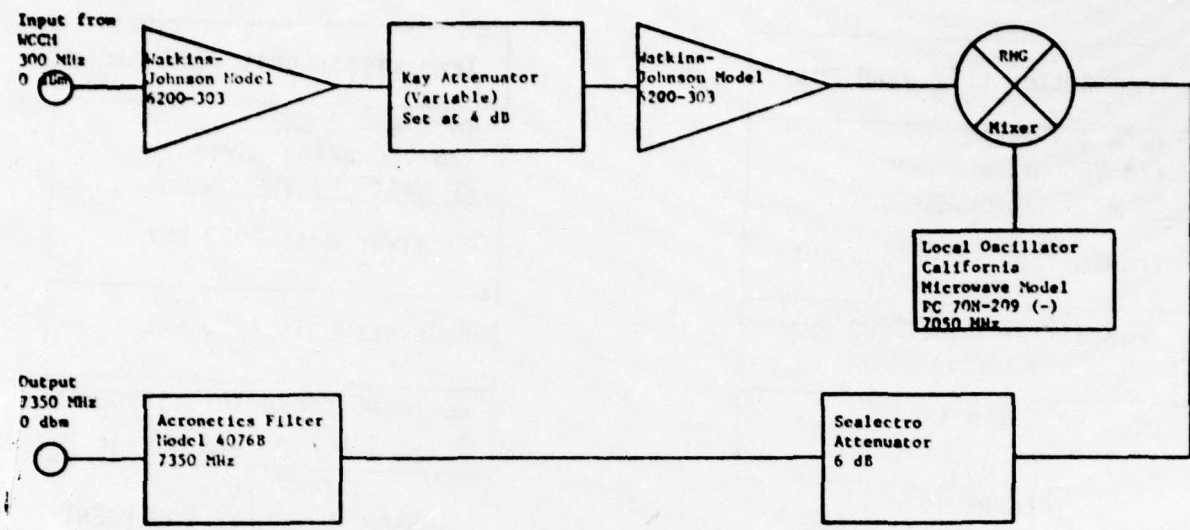


FIGURE 20 SENSOR TRANSMITTER 7350 MHz

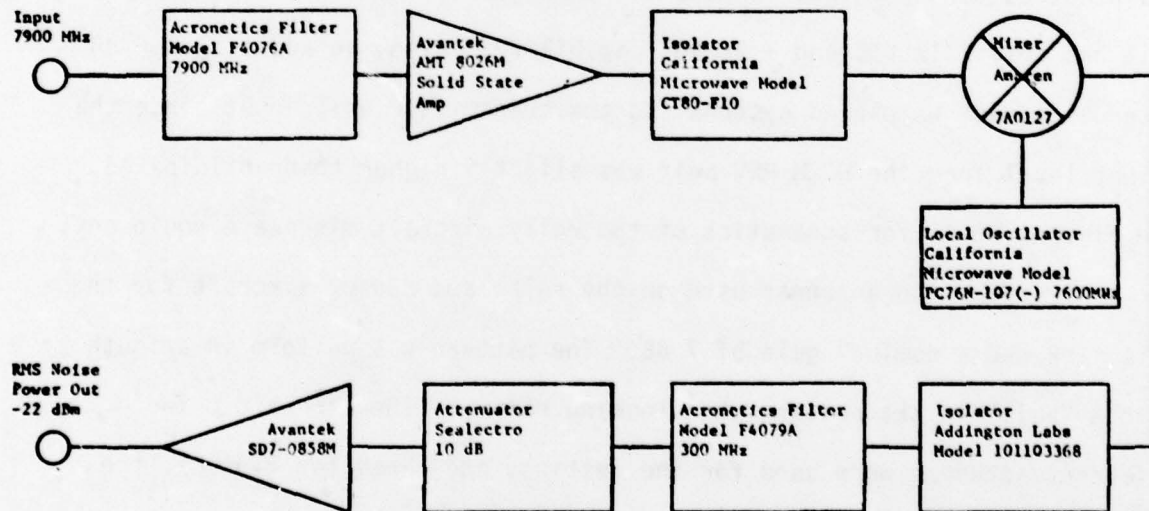


FIGURE 21 SENSOR RECEIVER 7900 MHz

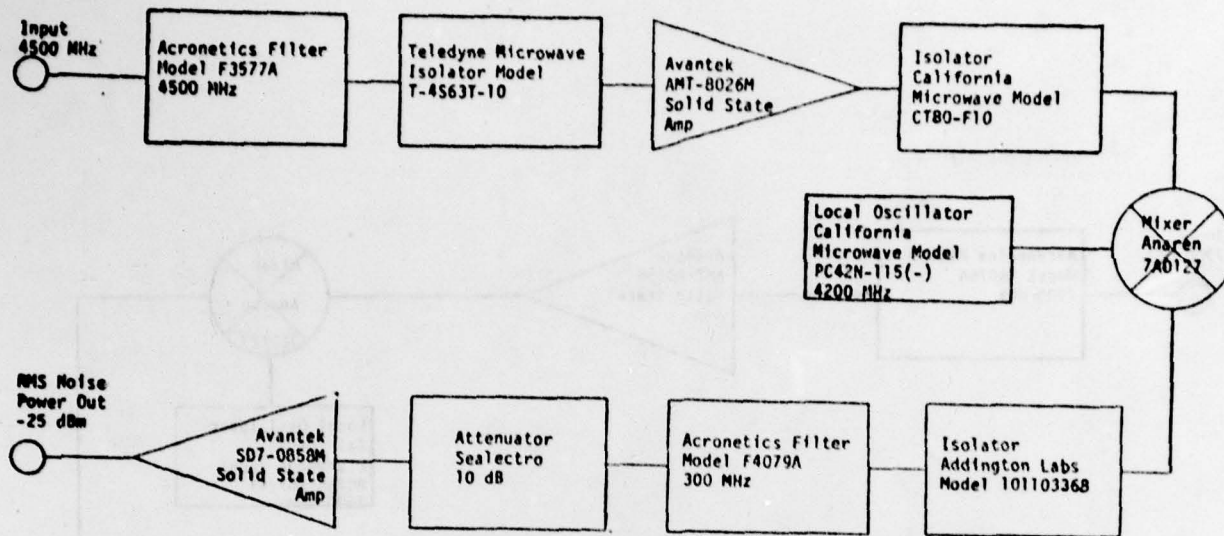


FIGURE 22 SENSOR RECEIVER 4500 MHz

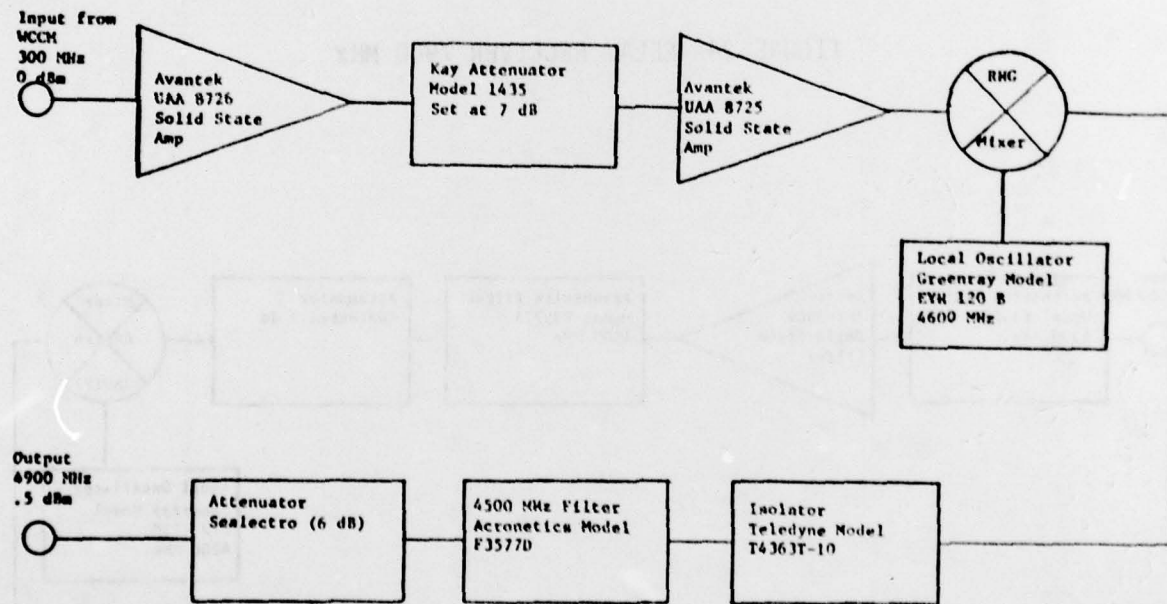


FIGURE 23 RELAY TRANSMITTER 4900 MHz

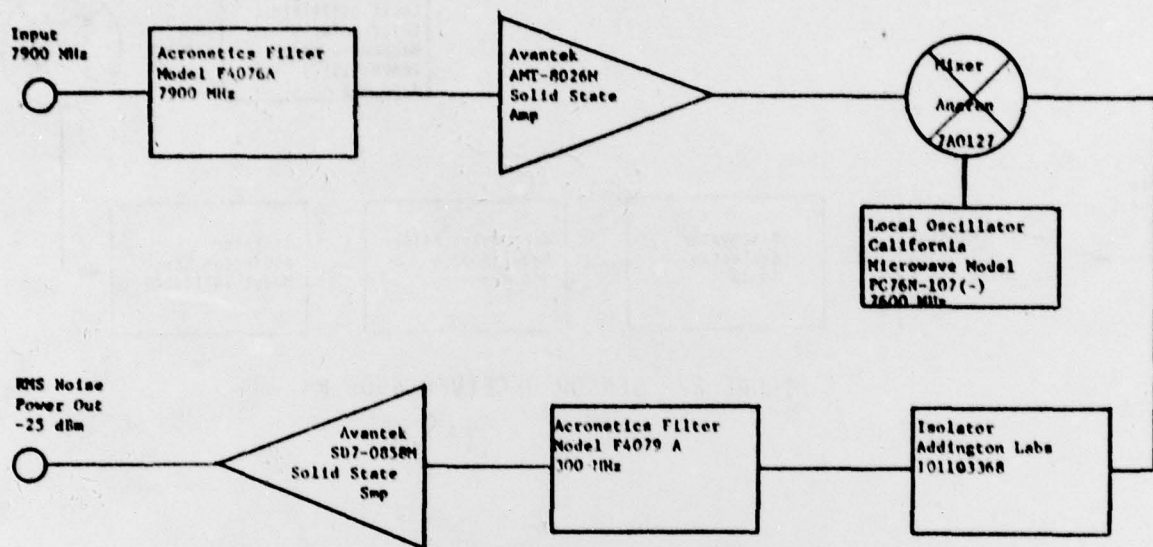


FIGURE 24 RELAY RECEIVER 7900 MHZ

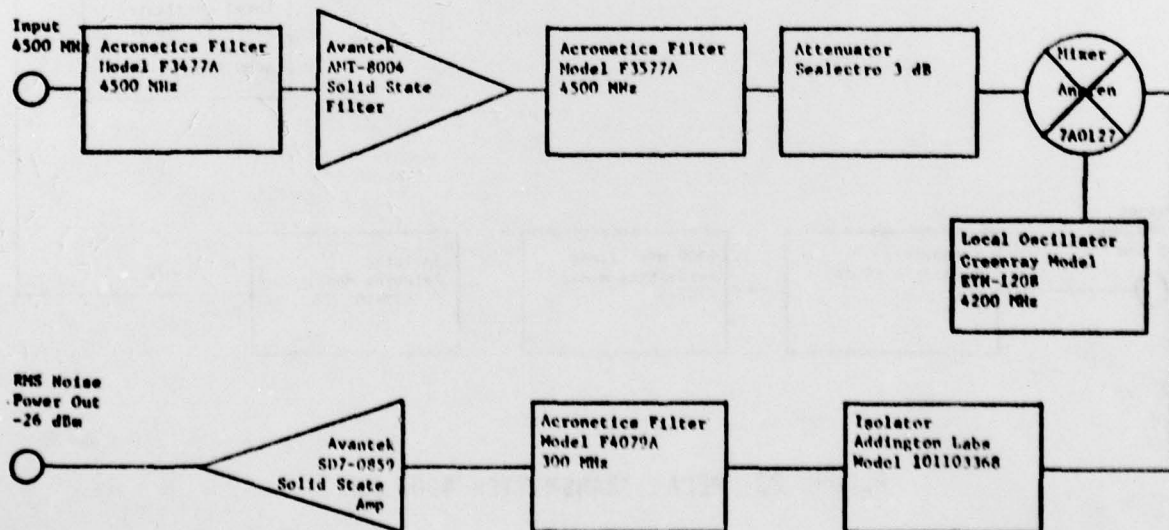


FIGURE 25 RELAY RECEIVER 4500 MHZ

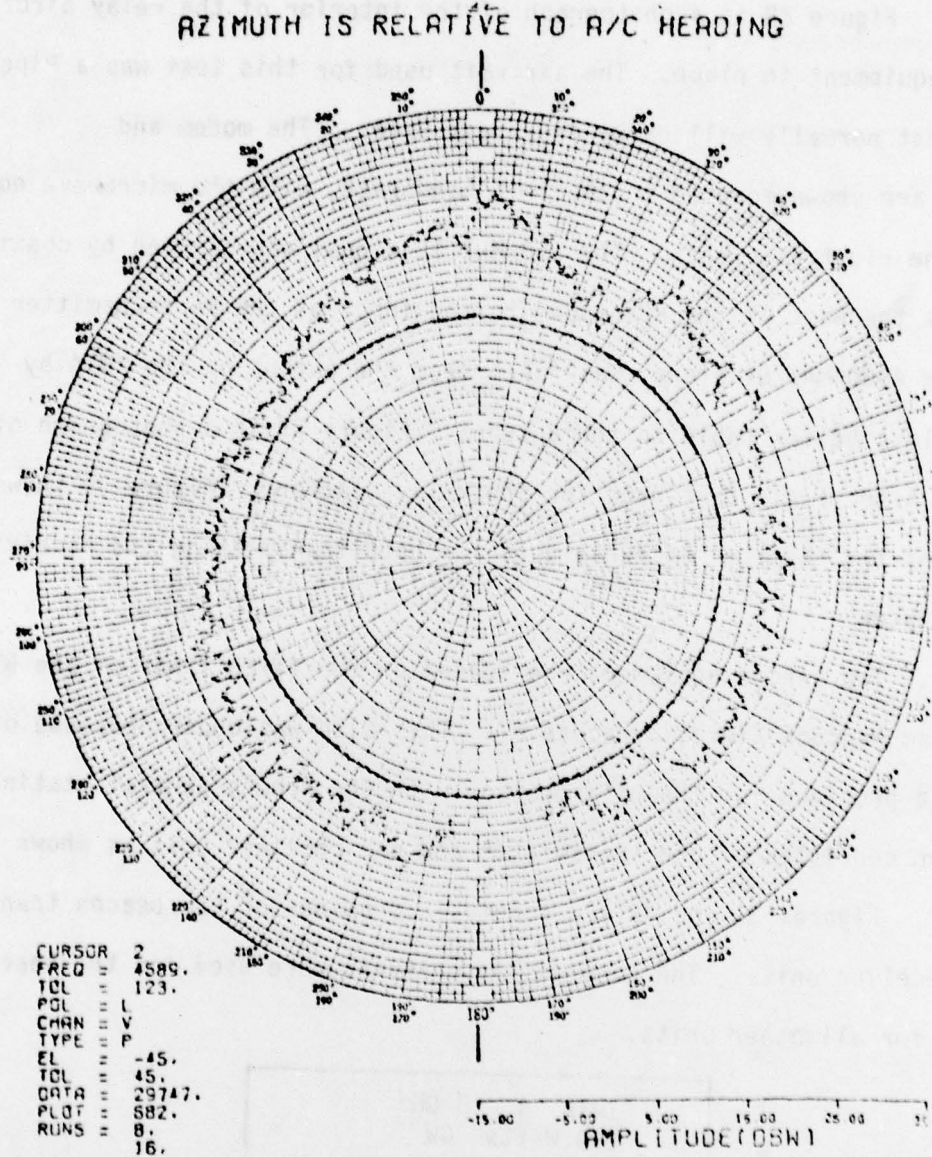


FIGURE 26 BUTTON ANTENNA PATTERN

3. Figure 28 is a photograph of the interior of the relay aircraft with the equipment in place. The aircraft used for this test was a Piper Aztec F that normally will carry four passengers. The modem and equipment are shown mounted in the left hand rack, with the microwave equipment in the right hand rack. The 300 MHz IF signal was carried by coaxial cable from the back of the RPV modem to the input of the RF transmitter unit. The 4900 MHz RF signal was taken from the output of the TWTA by very low loss heliax cable to the antenna. Figure 29 is a photograph of the Piper Aztec F aircraft used for the relay platform. Figure 30 shows a close-up of the "button" antennae used for both transmitting and receiving.

d. Beacon

1. The beacon equipment was housed on the fifth floor of the NORAD building at Hancock Field, Syracuse NY. This site was chosen because of the wide angle provided for the bilateration with the ground control station. The beacon consisted of one transmitter and one receiver unit as shown in Figure 27. Figures 31 and 32 are schematic drawings of the beacon transmitter/receiver units. The same design criteria were used for the beacon units as for all other units.

TWTA 4 - 8 GHz 200 Watts CW
Transmitter 4500 MHz
Receiver 4900 MHz
AC - DC Converter 120 VAC, 60 Hz in ± 12, + 28 VDC output

FIGURE 27 BEACON EQUIPMENT

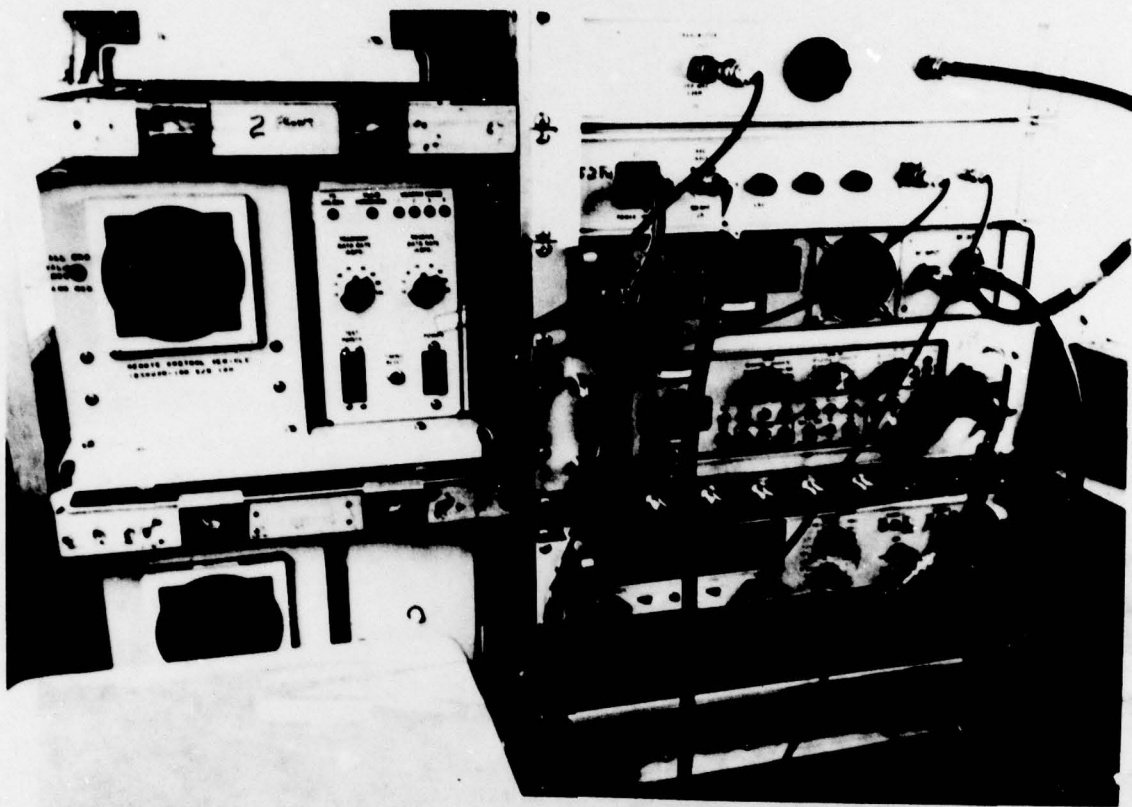


FIGURE 28 RELAY AIRCRAFT EQUIPMENT

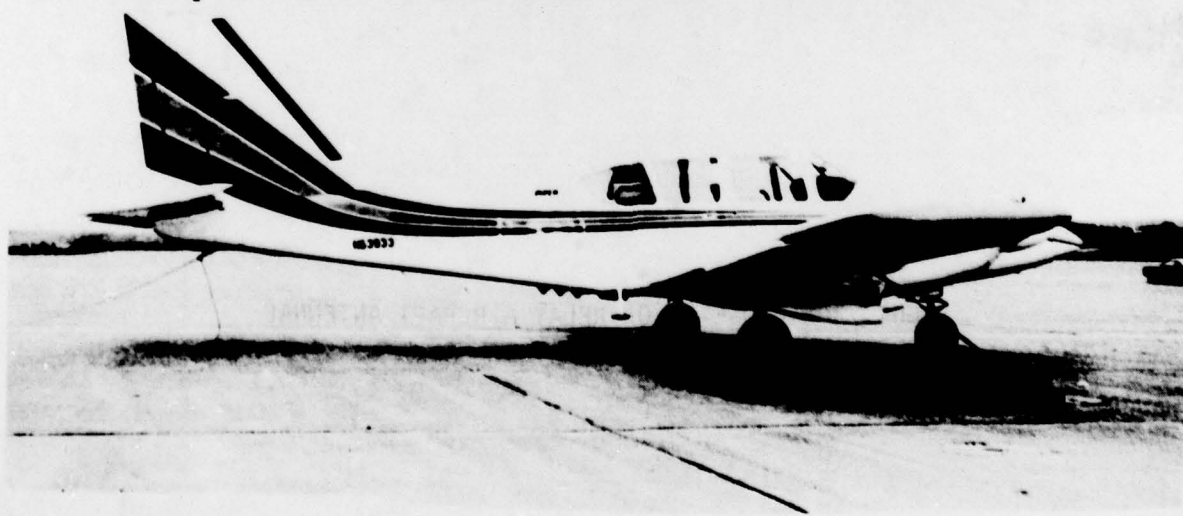


FIGURE 29 RELAY AIRCRAFT

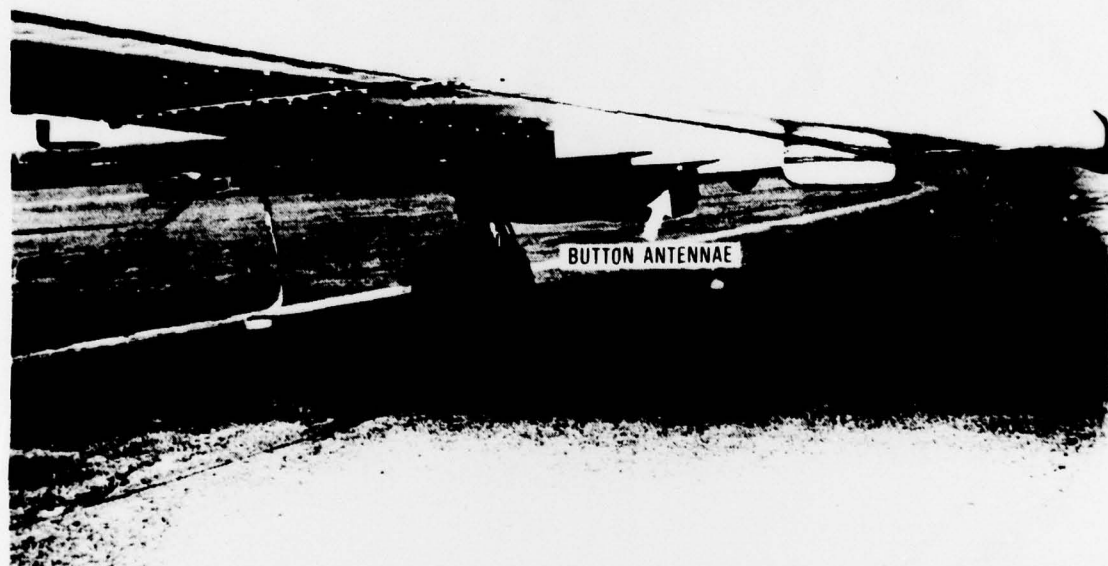


FIGURE 30 CLOSE-UP OF RELAY AIRCRAFT ANTENNAE

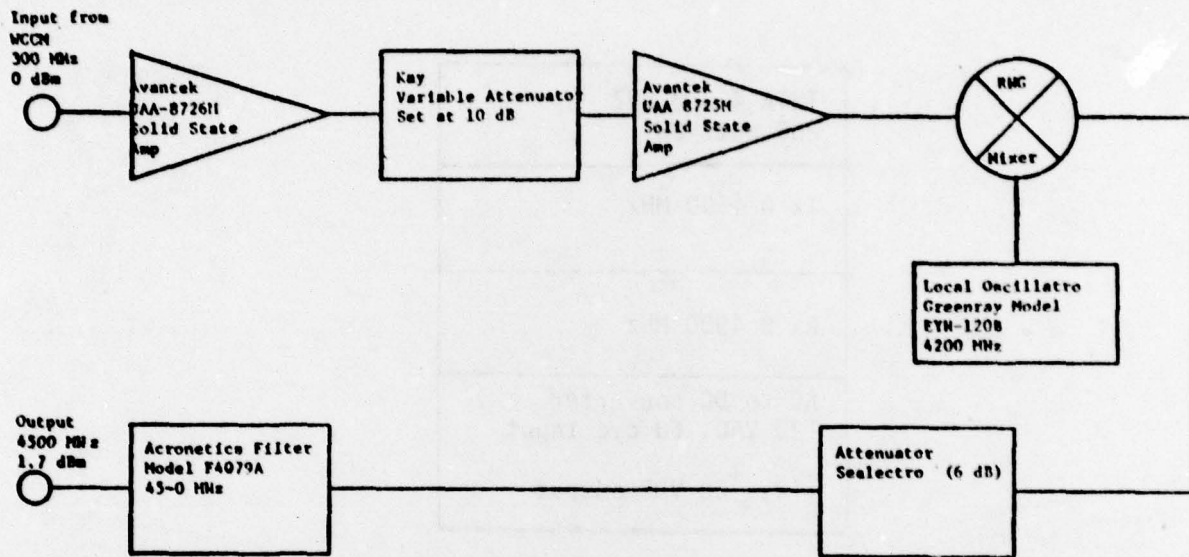


FIGURE 31 BEACON TRANSMITTER 4500 MHz

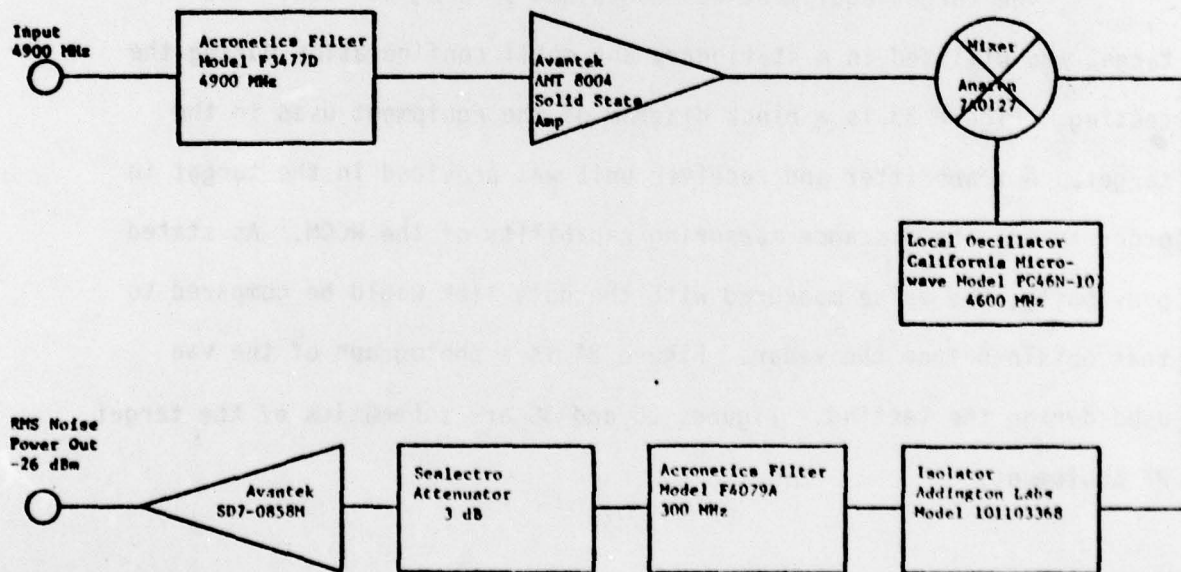


FIGURE 32 BEACON RECEIVER 4900 MHz

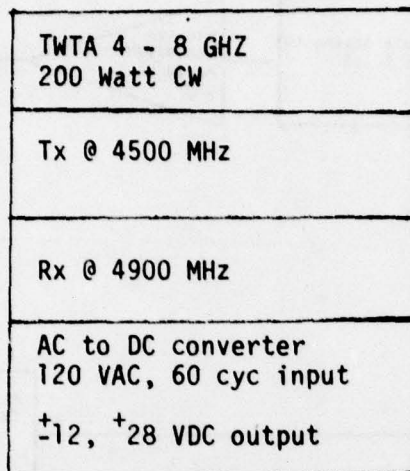


FIGURE 33 TARGET EQUIPMENT

5. Target

The target equipment was contained in a 2½ ton van. The target was utilized in a stationary and mobil configuration during the testing. Figure 33 is a block diagram of the equipment used in the target. A transmitter and receiver unit was provided in the target in order to use the distance measuring capability of the WCCM. As stated previously, the value measured with the data link would be compared to that obtained from the radar. Figure 34 is a photograph of the van used during the testing. Figures 35 and 36 are schematics of the target RF equipment.

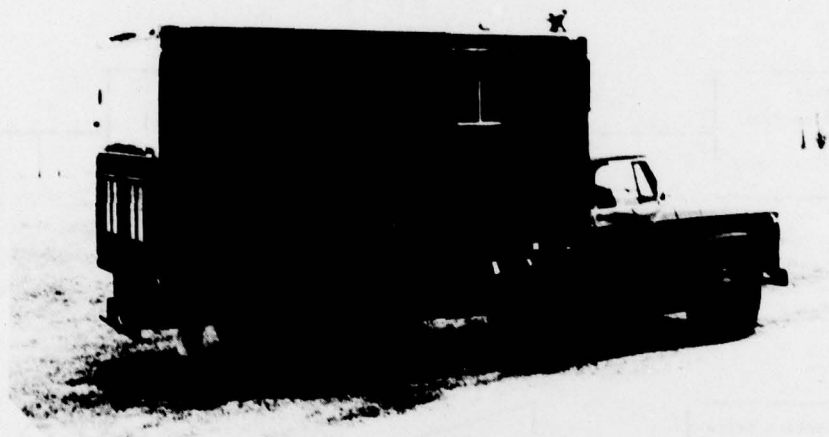


FIGURE 34 TARGET VAN

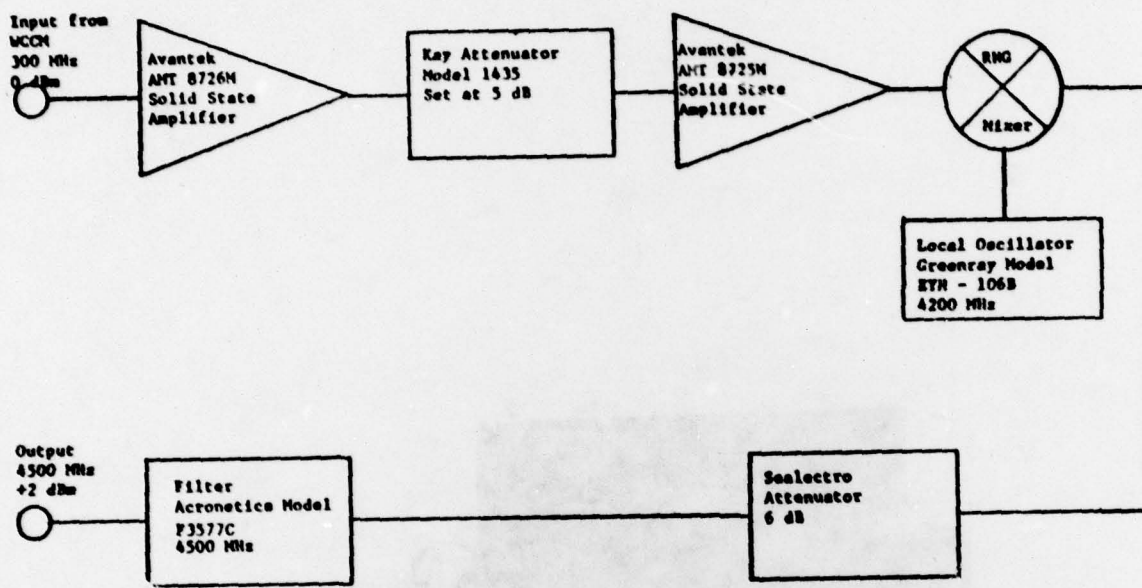


FIGURE 35 TARGET TRANSMITTER 4500 MHz

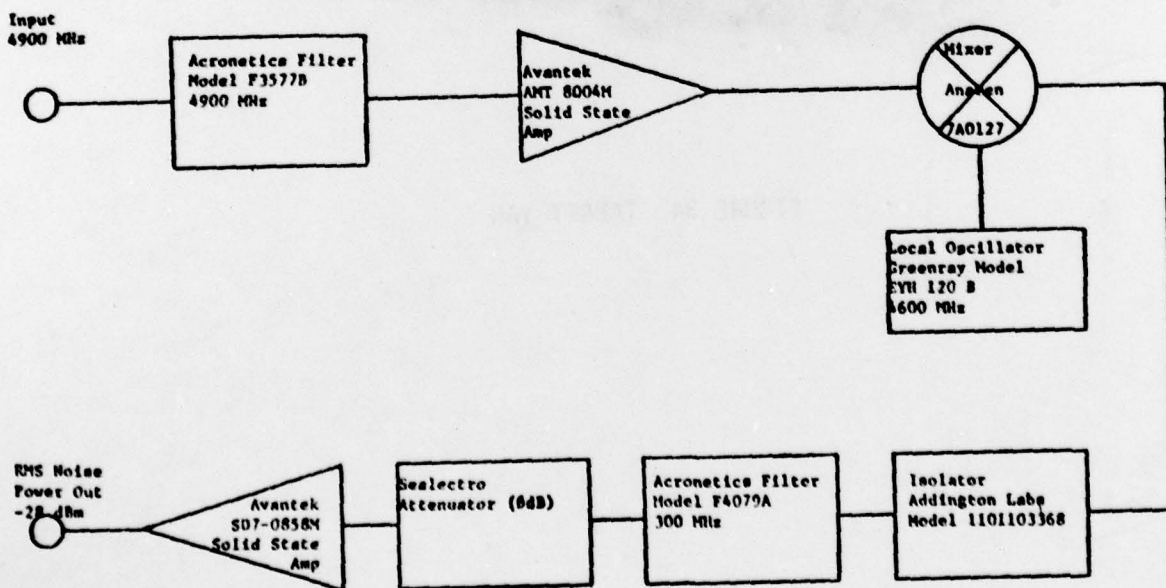


FIGURE 36 TARGET RECEIVER 4900 MHz

4. SUMMARY

4.1. The objectives of this technical report were to present the results of the flight testing of a wide bandwidth spread spectrum communications modem using a test facility developed in-house at the Rome Air Development Center. Although complete testing of the five station computer controlled communications link was pre-empted due to funding and time constraints, considerable flight testing was done which proved the ability of the modem to maintain communication at a BER of 10^{-6} at ranges within experimental expectation.

4.2 Section two of the report details the design goals for a typical flight scenario using a representative wide bandwidth spread spectrum modem built to RADC specifications by Hughes Aircraft Corporation of Fullerton, California. Equations are presented for determining the maximum range achievable from the standpoint of BER, estimated radiated power (ERP), system noise figure and antenna selection. For the Hughes Aircraft Corporation modem the maximum theoretical range achievable was determined to be over four hundred and fourteen miles. The differences in the ranges tabulated in table 1 (for the various links) are a function of the processing gain of the spread spectrum modem, with all other parameters being held constant, e.g. ERP, noise figure, bandwidth and antenna gain.

4.3 Section three outlines a five station test profile consisting of three ground terminals and two airborne terminals. One ground terminal was detailed as the ground control station where the entire flight test scenario could be controlled by two mini-computers. The airborne equipment

was designed to be flown in a controlled cabin environment of a low performance aircraft. Also, in this section the transmitter and receiver schematic drawings were presented and explained in sufficient detail to allow an unfamiliar operator to use the equipment to its optimum capability with little or no explanation.

4.4 It should also be noted here that the system has been flown in an operational scenario, with the ranges achieved being within experimental expectation of the theoretical calculations. As an example, the theoretical calculation for the command and control uplink from the GCS to the two airborne platforms was shown to be approximately ninety seven miles. In actual flight tests a maximum range of thirty-five miles was achieved at the required bit error rate. In the theoretical calculations the effects of multipath, atmospheric losses due to water vapor and transmitting and receiving antenna non-alignment were not taken into consideration. With this in mind the differences between the theoretical and flight test measured ranges are well within experimental expectation.

4.5 For future requirements the desired ranges could be increased substantially by placing the low noise pre-amplifiers and preselectors immediately after the receive antenna. This would provide a significant improvement in the system by making the losses due to long cable runs negligible. With this minor change the expected range could be increased by a factor of two or better.

5. REFERENCES

1. J. A. Kivet and G. F. Bowers, Wideband Command and Control Modem (Waveform and Modem Conceptual Design Study), Final Technical Report, RADC-TR-73-12, Dec 1972, AD 756 933.
2. M. J. Parrish, et al., MRS³ Test Data Link Modem Study, Final Technical Report, Hughes Aircraft Corporation, July 1977.
3. Proposal for Alternative Configuration of Large T-W Preamble IF Model, Exhibit E, Hughes Aircraft Corporation, 13 June 1977.
4. J. A. Kivett and E. A. Koist, Wideband Command and Control Modem (Experimental Model Phase) (U) Hughes Aircraft Corporation, December 1974.
5. M. I. Skolnik, Introduction to Radar Systems, McGraw-Hill Book Company, 1962.
6. Reference Data for Radio Engineers, Fifth Edition, Pg 22-41, March 1969.
7. W. A. Skillman, Lecture Notes for Introduction to Radar, Westinghouse-Baltimore School of Applied Engineering, 1971-1972.